DOI:10.16555/j.1006-8775.2014.03.008

Article ID: 1006-8775(2014) 03-0251-16

NUMERICAL EXPERIMENTS FOR THE EFFECTS OF TWO MODEL INITIALIZATION SCHEMES ON RAINFALL FORECAST IN THE 2008 FLOODING SEASON

WANG Ye-hong (王叶红), PENG Ju-xiang (彭菊香), ZHAO Yu-chun (赵玉春)

(Hubei Key Laboratory for Heavy Rain Monitoring and Warning Research, Institute of Heavy Rain, China Meteorological Administration, Wuhan 430074 China)

Abstract: In this paper, based on heavy rain numerical forecast model AREM (Advanced Regional Eta Model), two different initialization schemes, LAPS and GRAPES-3DVAR, are used to run assimilation experiments of AREM-LAPS and AREM-3DVAR with the same data source (NCEP forecast field, surface data and radio-soundings) during the period from 21 May to 30 July 2008 to investigate the effect of the two initialization schemes on the rainfall simulation. The result suggests that: (1) the forecast TS score by the AREM-LAPS is higher than that by the AREM-3DVAR for rainfall in different areas, at different valid time and with different intensity, especially for the heavy rain, rainstorm and extremely heavy rain; (2) the AREM-3DVAR can generally simulate the average rainfall distribution, but the forecast area is smaller and rainfall intensity is weaker than the observation, while the AREM-LAPS significantly improves the forecast; (3) the AREM-LAPS gives a better forecast for the south-north shift of rainfall bands and the rainfall intensity variation than the AREM-3DVAR; (4) the AREM-LAPS can give a better reproduction for the daily change in the mean-rainfall-rate of the main rain band, and rainfall intensity changes in the eastern part of Southwest China, the coastal area in South China, the middle-lower valleys of Yangtze river, the Valleys of Huaihe river, and Shandong peninsula, with the rainfall intensity roughly close to the observation, while the rainfall intensity simulated by the AREM-3DVAR is clearly weaker than the observation, especially in the eastern part of Southwest China; and (5) the comparison verification between the AREM-LAPS and AREM-3DVAR for more than 10 typical rainfall processes in the summer of 2008 indicates that the AREM-LAPS gives a much better forecast than AREM-3DVAR in rain-band area, rainfall location and intensity, and in particular, the rainfall intensity forecast is improved obviously.

Key words: weather forecast; precipitation characteristics; numerical experiment; flooding-season rainfall; LAPS system; GRAPES-3DVAR system; AREM model

CLC number: P435 **Document code:** A

1 INTRODUCTION

The AREM (Advanced Regional Eta-Coordinate Model) model is the first mesoscale rainstorm model with independent intellectual property rights in China developed by Yu et al.[1-4], which depicts the East Asian climatic characteristics in China and takes the large-scale orographic effect of the Qinghai-Tibetan Plateau into consideration. It has been widely applied in the research and operating agencies of meteorological, hydrological, environmental and military support at home and abroad, and is one of the main models for mesoscale rainstorm research and forecast in China[5-10]. After developing over more than a decade, AREM has progressed hugely. In addition to more standardized model structure, continuously improved model resolution, updated lateral boundary conditions, and more comprehensive physical process, the model's initialization schemes have been developed greatly. Besides the modified Barnes Scheme[4], the GRAPES-3DVAR three-dimensional variational data assimilation scheme[11] and the four-dimensional variational data assimilation scheme, which is based on historical sample projection technique (HSP_4dvar)[12], have been introduced and developed. Such continuous improvement in the initialization scheme gives an important impetus to improving the precipitation forecast level of the model. However, to date, the above assimilation systems still have limitations in

Received 2013-05-21; **Revised** 2014-04-29; **Accepted** 2014-07-15
Foundation item: Scientific Research Projects Specially for Public Welfare Industries (GYHY200906010); National Natural Science Foundation of China (41075034); Project 1009 for Wuhan Heavy Rain Institute
Biography: WANG Ye-hong, Professor, primarily undertaking research on data assimilation and mesoscale numerical simulation.
Corresponding author: WANG Ye-hong, e-mail: yehongw@whihr.com.cn

assimilating non-conventional data, which greatly restricts the effective application of a great deal of observation data in the model.

LAPS (Local Analysis Prediction System)[13, 14] is a local analysis and forecast system developed by Forecast Systems Laboratory under National Oceanic and Atmospheric Administration of USA (NOAA/FSL), which is able to effectively ingest many kinds of observation data from satellites, Doppler-radars, GPS (Global Positioning System), radio-soundings, automatic weather stations, wind profilers and microwave radiometers to produce high spatiotemporal resolution three-dimensional gridpoints analysis, is one of the most advanced local analysis systems worldwide nowadays. Now, LAPS is being widely applied in mesoscale meteorological data analysis[15, 16], nowcasting[17], numerical weather forecast through coupling with mesoscale models[18], among others. Outside China, a great number of real-time forecast and verification have been carried out on coupling of the LAPS system with models including RAMS (Region Atmosphere Model System)[19], MM5 (Mesoscale Model 5)[20], and WRF (Weather Research and Forecasting Model)[21], and their results indicate that LAPS may improve the quantitative short-term forecast effect by ingesting local data[20-21].

Since Wuhan Institute of Heavy Rain, China Meteorological Administration (WIHR/CMA) successfully transplanted LAPS in 2006[22, 23], China has successively carried out studies on combining LAPS and WRF. For instance, Li et al.[24] used LAPS to conduct comparative research of radar data assimilation in WRF and obtained fairly good results. The work to be urgently carried out is to study coupling techniques of AREM with LAPS, and then to investigate the model prediction effects and to compare the LAPS initialization scheme with the original one. Based on the work of previous researchers, we conducted a study on techniques of coupling LAPS with AREM, and compared this scheme with GRAPES-3DVAR scheme in an attempt to acquire the relative superiorities of both assimilation systems in summer precipitation forecast in China, so as to offer a basis for later professional researches.

Section 2 introduces the numerical model and initialization scheme. Section 3 describes the technique of coupling between model and LAPS. Section 4 gives a brief introduction to two experiments with different initialization schemes. In section 5, results of the two experiments are compared. Discussion and conclusions are provided in section 6.

2 MESOSCALE NUMERICAL MODEL AND INITIALIZATION SCHEME

We used the model AREMv2.3, of which the vertical coordinate is η-coordinate, the horizontal grid is on the E grid with the horizontal resolution of about 37 km on average, the vertical direction is divided into 35 layers at unequal distances, and the model top is at 50 hPa. The major physical processes of this model include nonlocal boundary layer, horizontal diffusion, warm cloud microphysical process, Betts convection parameterization adjustment scheme, and surface radiation parameterization based on the Benjamin theory. The surface flux is determined with the multiple stratified flux-profile method, while the water vapor advection is calculated with the positive definite conformal advection scheme. The time-varying boundary condition is adopted. The model integration range is 85°–135°E and 15°–55°N, and the time integral step is 225 s.

For initial value analysis, GRAPES-3DVAR[11], developed by Center for Numerical Prediction and Research, Chinese Academy of Meteorological Sciences, and LAPS, developed by NOAA/FSL, were used. The basic algorithm of LAPS is to use distance-weighted interpolation for the observation data based on the background field so as to obtain gridpoint values, and then to restrain the relationship between the surface wind and pressure using a two-dimensional variational method, the relationships among the temperature, pressure and wind at high levels using a three-dimensional variational method, and the vertical water vapor distribution using a one-dimensional variational method. WIHR/CMA has successfully transplanted LAPS to the local platform by modifying the data format and revising some parameters. At present, this system is being used to ingest the NCEP data, Doppler radars, satellites, surface data, radiosonde and GPS water vapor, among others, its real-time operational running is carried out, and its analysis products are released in real time on the website of WIHR/CMA (http://www.whihr.com.cn)[22].

3 COUPLING BETWEEN AREM AND LAPS

A great quantity of research results have been obtained from the coupling between AREM and GRAPES-3DVAR and related experiments, whereas there are fewer studies carried out on the coupling between AREM and LAPS, which will be intensively introduced in this section.

To couple LAPS with AREM so that the LAPS temperature, pressure, humidity and wind analysis fields can be initiated in the AREM model, one has to implement several techniques, including the LAPS domain setting, coordinate transformation, data format processing, and linking with the AREM model.

LAPS offers three projection modes, namely, polar stereographic projection (Plrstr), Lambert

projection (Lambrt), and Mercator projection (merctr). If the analyzed regions center on the polar region or high latitudes, then the polar stereographic projection is normally selected. If the analyzed regions are in the middle-to-high latitudes of the Northern Hemisphere, then Lambert projection is normally used. If the analyzed regions are on the equator or in a 1°–2° low-latitude tropical zone, then the Mercator projection is used. The regions of China analyzed in this paper are mainly in middle-to-high latitudes, so the Lambert map projection was chosen. LAPS adopts rectangular coordinate gridpoints for data analysis, and the center position and grid spacing of the analyzed region can be arbitrarily set depending on the requirement. The central point of the LAPS domain in this paper was chosen at 110°E/35°N with a horizontal resolution of 20 km and the number of gridpoints of 301×281. The LAPS analysis was converted from a rectangular coordinate mesh into a latitude/longitude coordinate mesh (Fig. 1). As the parallels of earth latitude differ in length, a rectangular region for data analysis in a rectangular coordinate mesh will be a fan-shaped area in latitude/longitude gridpoint coordinates; the lower the latitude, the smaller the area covered by the analysis, while the higher the latitude, the larger the area covered by the analysis. Because of the feature that the LAPS analysis field exhibits a fan-shaped distribution in a latitude/longitude coordinate grid, an appropriate LAPS domain must be set according to the model region so that the LAPS analysis can cover the model integration area. The rectangle shown by the black solid lines in Fig. 1 is the integration area of the AREM model and the LAPS domain chosen in this paper covers the entire model domain and thus can initialize AREM.

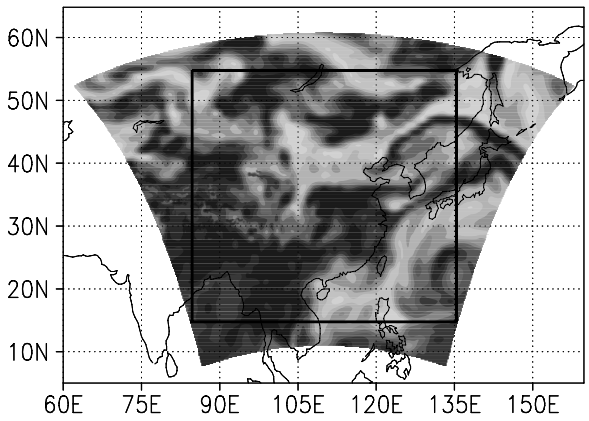

Figure 1. Schematic diagram of relative humidity distribution at 500 hPa from LAPS analysis at 08:00 July 22, 2008 (The rectangle shows the integration area of AREM model).

The LAPS analysis is of rectangular coordinate mesh, whereas the AREM model adopts a latitude/longitude coordinate mesh, thus, coordinate transformation must be done before realizing the coupling between LAPS and AREM. The GrADS Plotting Software directly offers a convenient tool for converting an LAPS analysis field from a rectangular coordinate mesh to a latitude/longitude coordinate mesh, thereby making the values of latitude/longitude grid coordinates within the required scope directly obtainable.

4 HINDCAST EXPERIMENT SCHEME

Exp. AREM-LAPS: The initialization scheme used LAPS, of which the background field was provided by the 12-h forecasts of the NCEP model, and the ingested observation data included the radiosonde and surface data.

Exp. AREM-3DVAR: Similar to Exp. AREM-LAPS, except that its initialization scheme used GRAPES-3DVAR.

For both of the above experiments, the model physical processes were completely consistent, and the lateral boundary conditions were updated every 6 h, using data from the NCEP forecasts. In addition, to reflect the influences of both of the initialization schemes on the precipitation prediction effect more objectively, both of the experiments adopted the analysis field of the same resolution, i.e., grid spacing of 1°×1°, to initiate the model. Obviously, the results of both of the above experiments can show the forecast difference arising from different initialization schemes.

The experiment period was from May 21 to July 30, 2008; the forecast was initiated at 08:00 and 20:00 every day (Beijing time, the same hereinafter) with a forecast validity period of 84 h. During the period, a total of six operation faults occurred at 20:00 June 2, 08:00 June 3, 20:00 June 24, 08:00 June 25, 20:00 July 19, and 20:00 July 20, due to data missing.

5 ANALYSIS OF HINDCAST EXPERIMENTAL RESULTS FOR FLOOD SEASON IN 2008

5.1 *Threat score results*

Firstly, the threat score (TS) was verified from the hindcast experimental results to have a general understanding of the influences of both of the initialization schemes on precipitation forecast. The precipitation verification method for National Meteorological Center of China[25, 26] and WIHR[27, 28] was employed. There were five rainfall thresholds (≥0.1 mm, ≥10 mm, ≥25 mm, ≥50 mm and ≥100 mm, i.e., light rain, moderate rain, heavy rain, torrential rain, and extremely heavy rain). The scoring regions were: all China (85°–135°E, 15°–55°N), the middle and lower reaches of the Yangtze River (110°–123°E, 25°–35°N), South China (105°–123°E, 18°–29°N), North China (110°–123°E, 35°–45°N), Northeast

China (120°–135°E, 40°–53°N), and the eastern part of Southwest China (100°–110°E, 20°–35°N). There were five time intervals tested for precipitation forecast: 0–24 h, 24–48 h and 48–72 h precipitation amounts predicted by the model with 08:00 as the initial time, and 12–36 h and 36–60 h precipitation amounts predicted with 20:00 being the initial time. For 400 basic gauging stations throughout China, we performed 24-h cumulative precipitation verification, used a distance-weighted average method to interpolate the model-predicted gridpoints precipitation amounts to gauging stations, and compared them against observed precipitation amounts at the respective gauging stations.

Figure 2 gives the TS score of 0-24 h precipitation forecast starting at 08:00 from May 21 to July 30 for the above six regions based on the AREM-LAPS and AREM-3DVAR experiments. After the initialization scheme was modified from GRAPES-3DVAR to LAPS, the TS scores at all thresholds rose to variable extents with respect to the all-China or the model domain (Fig. 2a), and the TS scores for light rain, moderate rain, heavy rain, torrential rain and extremely heavy rain rose by 2.3%, 3.7%, 4.1%, 2.9% and 2.6%, respectively, indicating that Exp. AREM-LAPS significantly improves the precipitation forecast results at all thresholds with respect to the average of the model domain. Besides, Exp. AREM-LAPS show characteristics that are obviously superior to those of Exp. AREM-3DVAR for various regions throughout China. As shown by Fig. 2b–2f, except for the light rain, torrential rain, and extremely heavy rain in the middle and lower reaches of the Yangtze River where the scores slightly fall (by 0.4%–0.6%), the TS scores for all thresholds in other regions increase by variable extents (by 0–8.5%). The TS scores increase most significantly in the eastern part of Southwest China, with the TS scores for light rain, moderate rain, heavy rain, torrential rain and extremely heavy rain up by 2.6%, 8.5%, 5.8%, 6.4% and 8%, respectively. Hence, the precipitation prediction was significantly improved for all thresholds, particularly for extremely heavy rain.

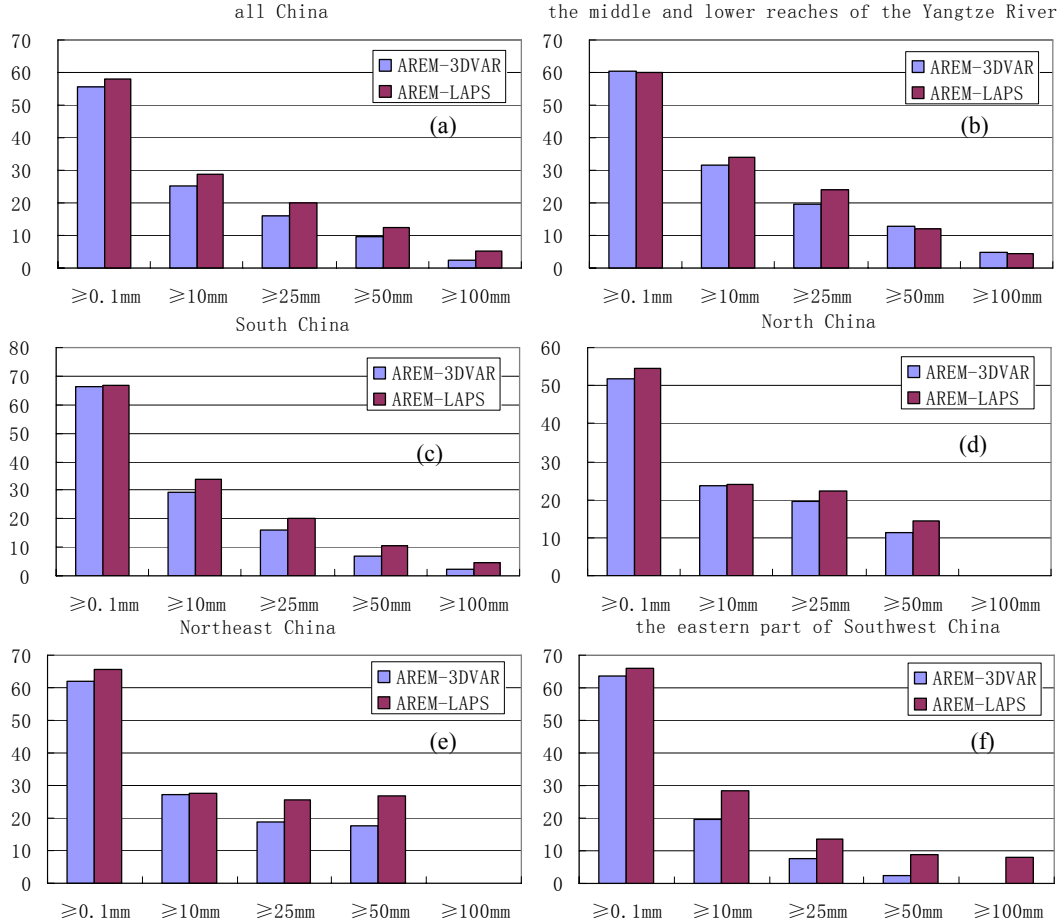

Figure 2. Model-predicted 0–24 h precipitation forecast TS scores from May 21 to July 30, 2008 (unit: %). Light and dark columns are the results of AREM-3DVAR and AREM-LAPS experiment, respectively. a. All China; b. the middle and lower reaches of the Yangtze River; c. South China; d. North China; e. Northeast China; f. the eastern part of Southwest China.

For the precipitation forecast for the other four time intervals, the TS score test was also conducted.

As the forecast validity period extends, the TS scores for various regions no longer exhibit the phenomenon that the AREM-LAPS experimental results are higher than the AREM-3DVAR experimental results, which are consistently reflected by the 0–24 h forecast results. Nevertheless, a total of 130 TS score differences in the above six regions at five precipitation thresholds and five forecast time intervals (Fig. 3, AREM-LAPS values minus AREM-3DVAR values) mainly exhibit positive values (70% positive, 23% negative, 7% zero), indicating that in most cases, the precipitation prediction effect of Exp. AREM-LAPS is better than that of Exp. AREM-3DVAR. Further regional investigation revealed that (Table 1), except Northeast China where the TS score rising frequency (8 times) is slightly less than the TS score dropping frequency (11 times), the total TS score rising frequency is much greater than the total TS score falling frequency in the case of all China, the middle and lower reaches of the Yangtze River, South China, North China and the eastern part of Southwest China, and the average increasing magnitude of the TS scores for each region is much greater than the average decreasing magnitude, indicating that Exp. AREM-LAPS obviously improves, in most cases, the precipitation prediction effects in various regions, at various thresholds and validity periods.

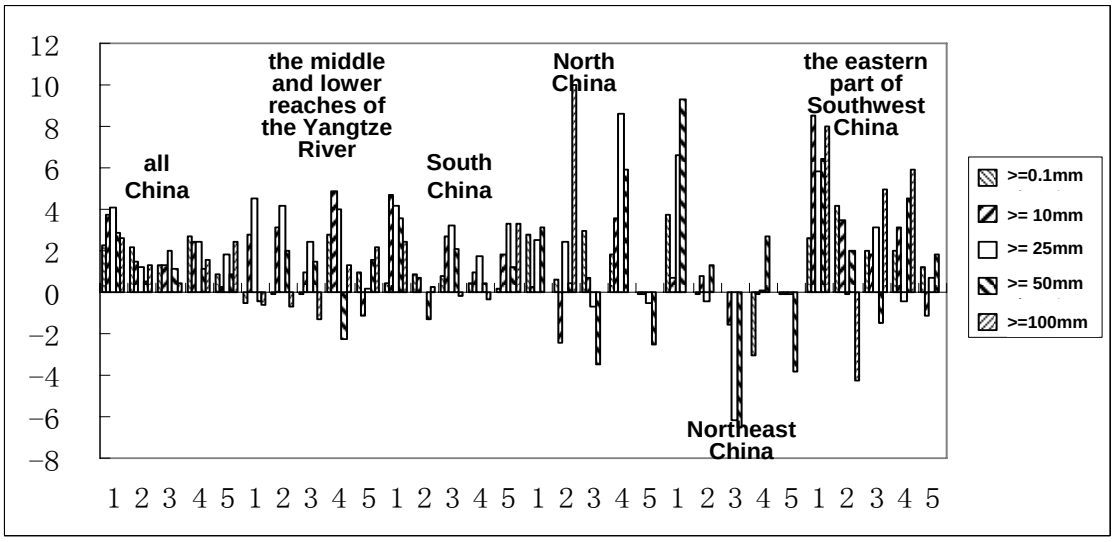

Figure 3. Distribution of TS score differences of AREM-LAPS experiment values minus AREM-3DVAR experiment values (%). Abscissas 1–5 represent 0–24 h, 12–36 h, 24–48 h, 36–60 h, and 48–72 h TS score difference series for each region respectively; ordinates are for the TS score differences.

Table 1. Distribution of TS score differences (%) of Exp. AREM-LAPS minus Exp. AREM-3DVAR for various regions.

Item	All China	The middle and lower reaches of the Yangtze River	South China	North China	Northeast China	The eastern part of Southwest China
TS score rising Total frequency/increasing magnitude	25 times/1.8%	16 times/ 2.47%	22 times/ 1.87%	14 times/ 3.26%	8 times/ 3.15%	19 times/ 3.79%
TS score falling Total frequency/decreasing magnitude	0 time	9 times/ -0.79%	3 times/ -0.61%	7 times/ -1.4%	11 times/ -2%	5 times/ -1.48%
TS score unchanged	0 time	0 time	0 time	4 times	6 times	1 time

To some extent, TS scores can help understand the overall difference between two initialization schemes in precipitation forecast in different regions and at different thresholds, but fail to give detailed differences in shape, location, intensity, precipitation center and temporal evolution characteristics of rain belts. Hereafter, the test results of both initialization schemes will be further compared.

5.2 *Daily mean precipitation rate from May 22 to July 30*

Comparisons between the observed daily mean precipitation rate from May 22 to July 30 (Fig. 4a, plotted with the 24-h rainfall from all China conventional rain gauging stations on the MICAPS, similar hereinafter) and the simulation of both experiments show that, rainfall areas and intensity simulated with Exp. AREM-3DVAR (Fig. 4c) are smaller, whereas Exp. AREM-LAPS (Fig. 4b) evidently improves this and reproduces fairly well the precipitation areas in the eastern China region, particularly the main rain areas in Guangxi,

Guangdong, Fujian, Jiangxi and the Yangtze River Delta, where the precipitation intensity from the experiment is equivalent to or slightly stronger than the observation; however, the AREM-LAPS precipitation simulation still shows weaker results in the Southwest China region (Yunnan, Guizhou, Sichuan, Chongqing), and some regions of Northeast China and North China.

It is worthwhile to note that, the daily mean precipitation rates (Fig. 4b) predicted by Exp. AREM-LAPS gives two strong precipitation centers with very small horizontal scale in the vicinity of Southwest Hubei (110°E, 30°N) and Central Hunan (111°E, 28°N), respectively, of which both the area and intensity are obviously greater than the observation. However, a Distribution Map of Mean Annual Precipitation in China (map omitted) shows that, both of the above regions, Yichang of Hubei and Xuefeng Mountain of Hunan, are each a precipitation center with small horizontal scale, probably due to the local topographic effect. As Fig. 4a is plotted with the MICAPS data from conventional rain gauging stations, it might not be able to reflect completely the meso- and micro-scale characteristics of precipitation distribution. Whether Exp. AREM-LAPS gives strong forecasts in both of the above regions or fails to truly show the meso- and micro-scale characteristics of precipitation due to sparse conventional gauging stations needs to be validated in the future using precipitation data with higher spatial resolution.

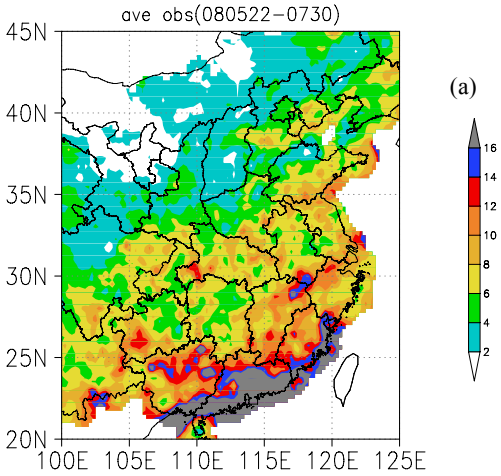

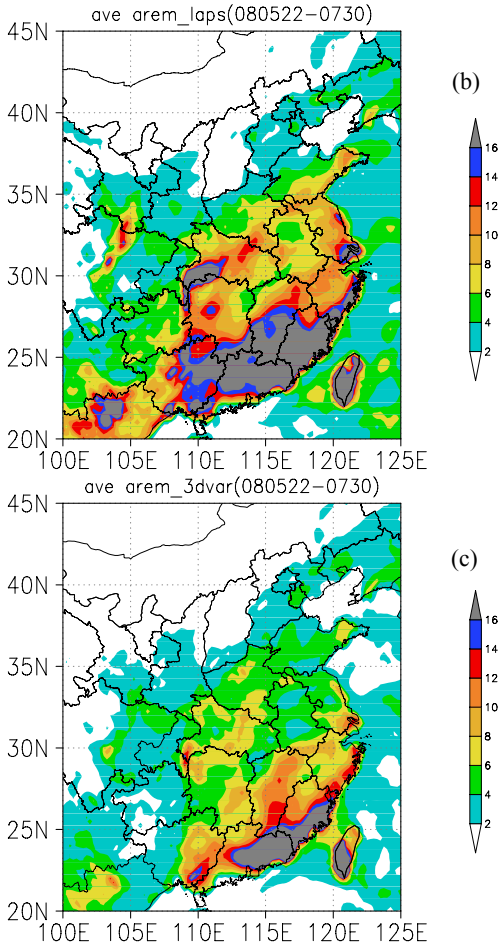

Figure 4. Daily mean precipitation rates of eastern China region from May 22 to July 30, 2008; a. Observation; b. Exp. AREM-LAPS; c. Exp. AREM-3DVAR. Unit: mm/d.

5.3 *Temporal evolution of regional average precipitation*

In the flood season of 2008, rainstorms occurred frequently in the eastern China region, resulting in abundant precipitation. Fig. 5a shows how the real average precipitation distributes over the 105°–123°E zone that evolved with latitude and time during a period from May 22 to July 30, 2008. From May 26 to 31, the precipitation over the region mainly distributed south of 35°N. In June, rain belts mainly centered on the south of 30°N, particularly the South China coastal area south of 25°N, instead of the obvious "northward uplifting" feature shown in normal years. From June 6 to 18, due to the effect of a quasi-stationary front in South China, persistent rainstorms occurred in Guangdong and Guangxi, resulting in regional flood disasters over the region. On June 20, as the western Pacific subtropical high intensified and shifted northward, the rain belt was moved northward to the Yangtze-Huaihe region, and the precipitation weakened and disappeared over South China. From June 25 to 30, as the tropical storm Fengshen (0806) landed on Guangdong, the western Pacific subtropical high retreated

southeastward, the rain belt disappeared over the Yangtze-Huaihe region, and rainstorms attacked South China and the area south of the Yangtze River again[29, 30]. In July, there were obviously more rainstorms in the north, and strong precipitation belts generally ran in a northeast-to-southwest direction and extended over thousands of kilometers, sometimes all the way from Northeast China to South China or Southwest China, and extremely heavy rain occurred successively in Northeast China, North China, Yangtze-Huaihe region, West China, South of Yangtze River and South China, while rainstorms hit Shandong Peninsula, the Yangtze-Huaihe region, the middle reaches of the Yangtze River and the southwest China region for several times.

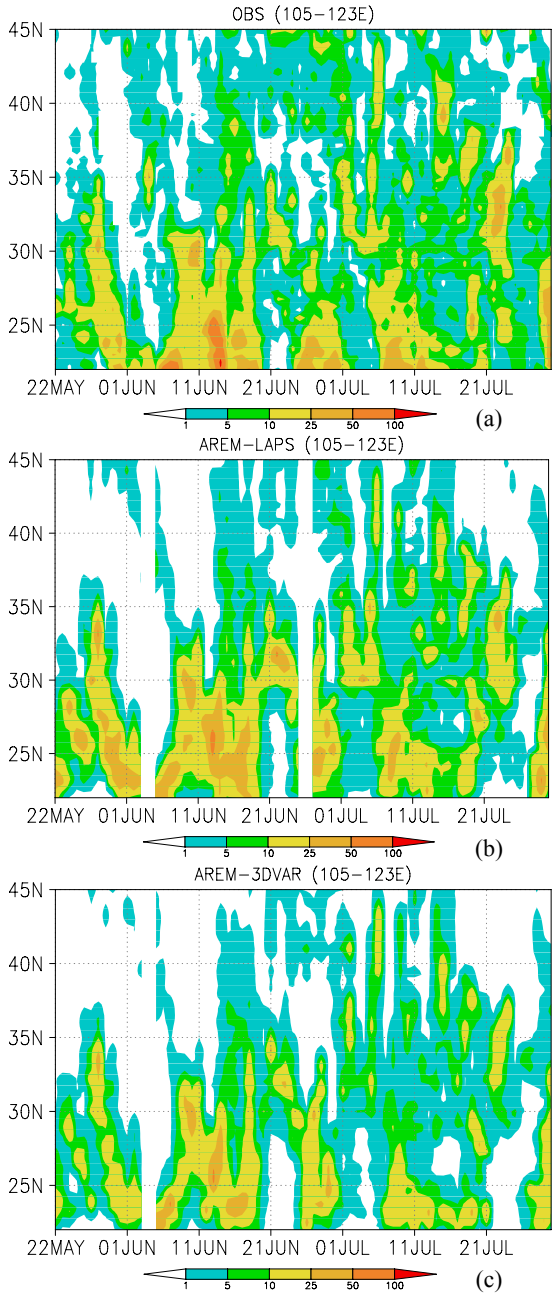

Figure 5. The time-latitude cross section of daily precipitation averaged in 105°–123°E from May 22 to July 30, 2008 (The captions are the same as in Fig. 4).

Exp. AREM-LAPS (Fig. 5b) simulates fairly well the rain belt distribution and its overall evolution characteristics, and the simulated process of north-to-south precipitation change basically agrees with the observation, with intensity being roughly comparable to the observation. Notably, despite that Exp. AREM-LAPS did a fairly good job in simulating the evolution tendency of the overall rain belt, the simulated rain belt over the South China region shifted much northward with weaker intensity and the simulated precipitation over northern China north of 35°N appeared weak, too. The simulation results of the AREM-3DVAR experiment (Fig. 5c) are inferior to those of the AREM-LAPS experiment; the former shows weaker intensity even though it also simulated the north-to-south rain belt change process. In addition, Exp. AREM-3DVAR exhibited the characteristic of the simulated South China rain belt shifting northward too, which implies that such northward shift is not caused by the initial field, but is probably related to the performance of the AREM model itself.

To further understand the model simulation of daily precipitation change in major precipitation zones, we divided the major rain areas into the eastern part of Southwest China (100°–110°E, 21°–34°N), South China (105°–120°E, 21.5°–25°N), the middle and lower reaches of the Yangtze River-the Huaihe River Basin (113°–122°E, 26°–34°N) and Jiaodong Peninsula (115°–123°E, 34°–39°N), according to the distribution of average precipitation over China from May 22 to July 30 as shown in Fig. 4a. Fig. 6 gives the time series of the observed and model-hindcast daily mean precipitation rates over these four regions.

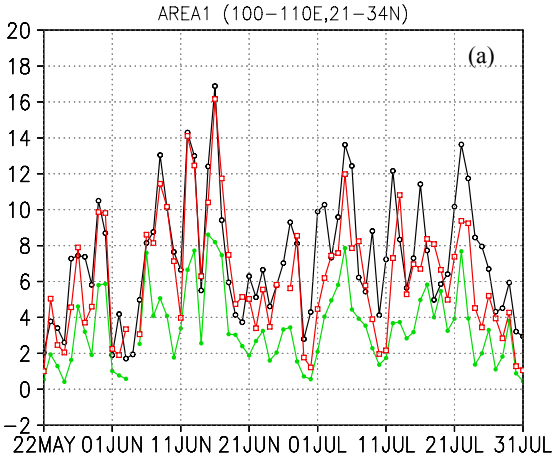

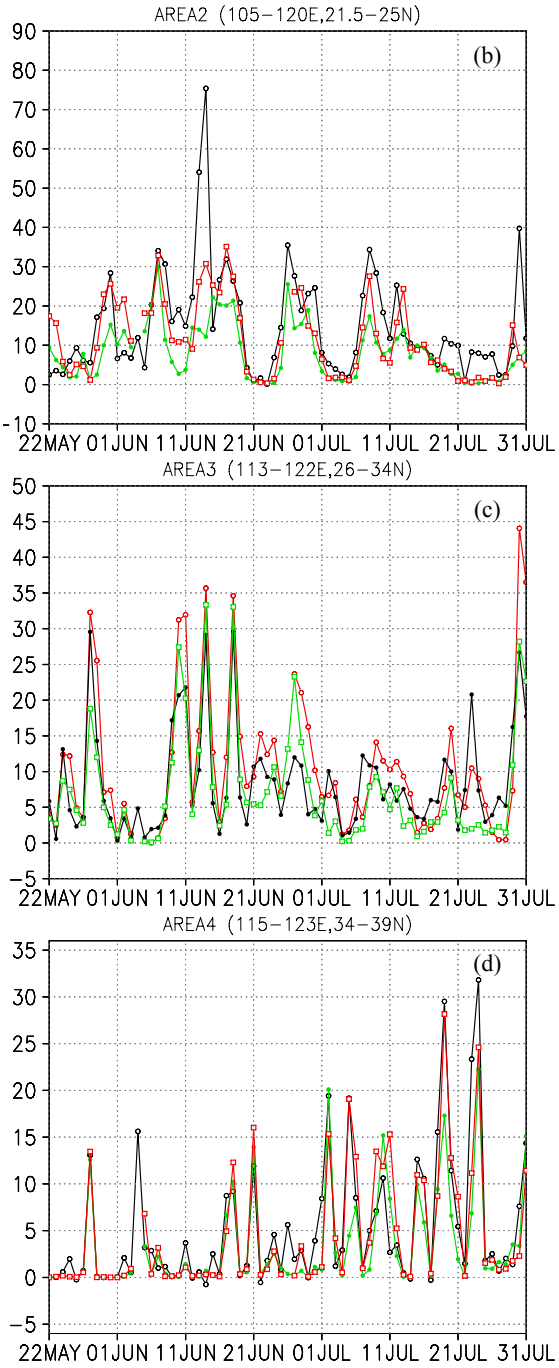

Figure 6. Time series of regional mean daily precipitation rates. a. eastern part of Southwest China; b. South China coastal area; c. middle and lower reaches of the Yangtze River to the Huaihe River Basin; d. Jiaodong Peninsula. Unit: mm. Black, red and green solid lines represent the observation, Exp. AREM-LAPS and Exp. AREM-3DVAR, respectively.

As seen from Fig. 6, the AREM-LAPS simulation of daily mean precipitation rates over the above four zones is generally superior to the AREM-3DVAR simulation. (1) The daily mean precipitation rate over the eastern part of Southwest China simulated by AREM-3DVAR is obviously weaker; the highest observed rate is 17 mm/d, whereas the strongest simulation is merely 8 mm/d, and the simulated daily mean precipitation rates are generally 50% or lower than the observation. The AREM-LAPS simulated precipitation rates (with a maximum of 16 mm/d) are roughly close to the observation, in particular several strong precipitation processes from May 22 to June 28 were accurately simulated, and their evolution tendencies and intensity are very close to the observation. (2) South China was a main precipitation and flooding zone in China during the flood season of 2008; its daily mean precipitation rate was much greater than that of the eastern part of Southwest China, with peak precipitation rates being generally as high as 30 mm/d or more, and even up to 76 mm/d on June 14. The AREM-3DVAR was able to simulate the South China precipitation evolution tendency, but the intensity was much weaker. The AREM-LAPS improved the precipitation intensity forecast and had fairly good simulation capability for strong precipitation at 20–30 mm/d, but still had weaker simulation for strong precipitation at more than 40 mm/d. (3) In the middle and lower reaches of the Yangtze-Huaihe Rivers basin, the main rain belts were relatively complex, the AREM-LAPS had insignificant improvement in forecasts, and the simulated precipitation rates were generally greater than the observation, thus Exp. AREM-LAPS might have overforecast for this zone. (4) Compared with Exp. AREM-3DVAR, Exp. AREM-LAPS improves in precipitation forecast for Jiaodong Peninsula, which still mainly shows in improved simulation of precipitation intensity.

Exp. AREM-LAPS reproduced very well the enhancing and weakening processes of daily mean precipitation rates in these four zones, and the simulated daily mean precipitation intensities were basically consistent with the observations; for each of the zones, Exp. AREM-LAPS improved all precipitation forecast results as compared with Exp. AREM-3DVAR, especially in terms of regional average precipitation intensity. We are always devoted to improving the numerical forecasting capability for torrential rains, extremely heavy rain and even extraordinary rainstorms, but how to improve the numerical forecasting accuracy of precipitation at torrential rain magnitude or above is always a major difficult problem facing meteorologists; the batch experiment results in this paper indicate that improvement in data assimilation techniques and assimilation systems has enormous potential for enhancing the forecast capability for strong precipitation.

5.4 *Typical rainstorms from May to July, 2008*

Rainstorms occurred frequently in China from May 22 to July 30, 2008. Comparative tests were carried out for more than ten typical precipitation processes in China occurring during this period, and the results show that, Exp. AREM-LAPS can forecast

the area, location and intensity of rain belts better than Exp. AREM-3DVAR, especially for local strong precipitation processes.

5.4.1 EXTRAORDINARY RAINSTORM IN SOUTHERN CHINA ON JUNE 9

On June 9, due to the influence of a 500-hPa trough and a mid-lower level intensive shear, an extensively strong precipitation process occurred in Guangxi and Hunan and the junction between Hubei, Anhui, Jiangxi and Zhejiang provinces, and the centers of two strong rainstorms were located at Tunxi in southern Anhui (24-h rainfall being 182.9 mm) and Luocheng in northwestern Guangxi (24-h rainfall being 155 mm). See Fig. 7.

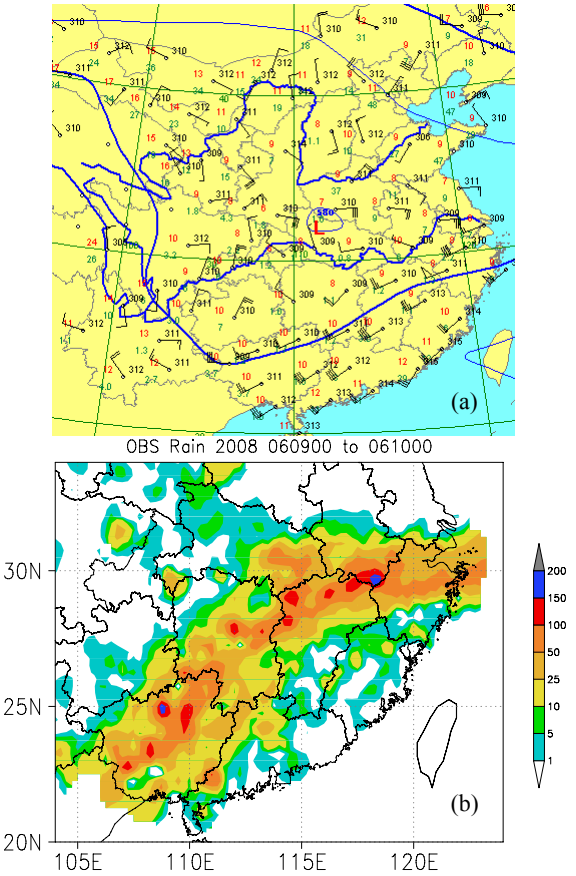

Figure 7. 700-hPa weather pattern at 08:00 June 9, 2008 (a) and 24-h cumulative precipitation at 08:00 June 10, 2008 (b, unit: mm).

Exp. AREM-3DVAR (Fig. 8a) simulated a northeast-to-southwest rain belt covering southern Jiangsu, southern Anhui, Zhejiang, southeastern Hubei, major part of Jiangxi, southern Hunan, and eastern Guangxi, whose location and orientation were fairly close to the observation, but it failed to simulate the rain area in Guangxi. Exp. AREM-LAPS (Fig. 8b) greatly improved the simulation of the entire rain belt, and successfully simulated a northeast-to-southwest rain belt, whose area and intensity were closer to the observation.

Comparisons of 700-hPa wind fields and 500-hPa geopotential height fields after 12-h integration between Exp. AREM-LAPS and AREM-3DVAR show that, there was obviously a shear existing in the Yangtze River Basin at 20:00 June 9, which was simulated by both experiments, but the intensity of the shear simulated by Exp. AREM-3DVAR is obviously weaker (Fig. 9). Furthermore, in reality, an obvious cyclonic shear existed in Guizhou and Guangxi, but the 700-hPa wind field simulated by Exp. AREM-3DVAR has a very weak shear here. In fact, the 700-hPa wind field over the whole Guizhou was northeasterly wind, whereas in the AREM-3DVAR experiment, westerly wind prevailed over Guizhou. Exp. AREM-LAPS successfully simulated the shear over the Yangtze River Basin with intensity close to the observation, and also successfully simulated the northerly wind and cyclonic shear within Guizhou. Differences in the simulation of weather pattern between both experiments directly lead to the discrepancies in the size and intensity of the rain belts simulated.

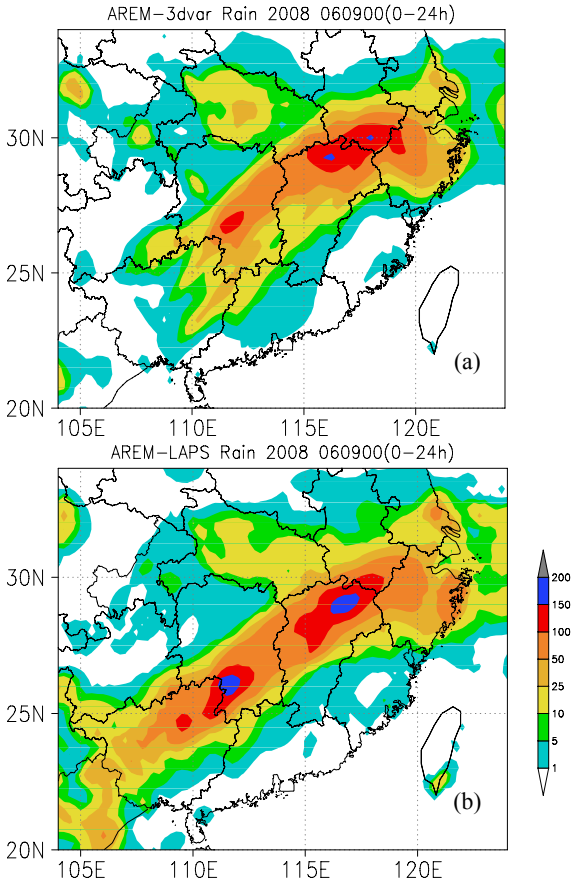

Figure 8. 24-h precipitation on June 10, 2008 simulated by Exp. AREM-3DVAR (a) and AREM-LAPS (b), respectively (Unit: mm).

5.4.2 VORTEX RAINSTORMS OVER SOUTH CHINA FROM JUNE 11 TO 14

On June 11, affected by the eastward movement of the southwest vortex, the precipitation belt was

enhanced in Yunnan, Guizhou and Guangxi, where rainstorms occurred at a total of 35 gauging stations; the precipitation was especially violent in Guangxi, and an extraordinary rainstorm occurred at one gauging station there (Donglan Station, 212.3 mm); on June 12, the rainstorm zone moved eastward and expanded its area, and the rainstorm occurred at a total of 111 gauging stations in the south of the Yangtze River and South China, including local extremely heavy rain in the northern and eastern parts of Guangxi, southern Hunan, southern Jiangxi, the northern and central-to-northern parts and coastal area of Guangdong, and extraordinary rainstorm in the central and northern parts of Guangxi and the estuary of the Pearl River. On June 13, the strong precipitation belt moved eastward and changed its direction to southwest-northeast due to the influence of an upper-level trough moving eastward in the north, and extremely heavy rain mainly occurred in the coastal area of South China, northern Guangdong, northern Jiangxi and some areas of southern Jiangxi. On June 14, the precipitation subsided[29, 30].

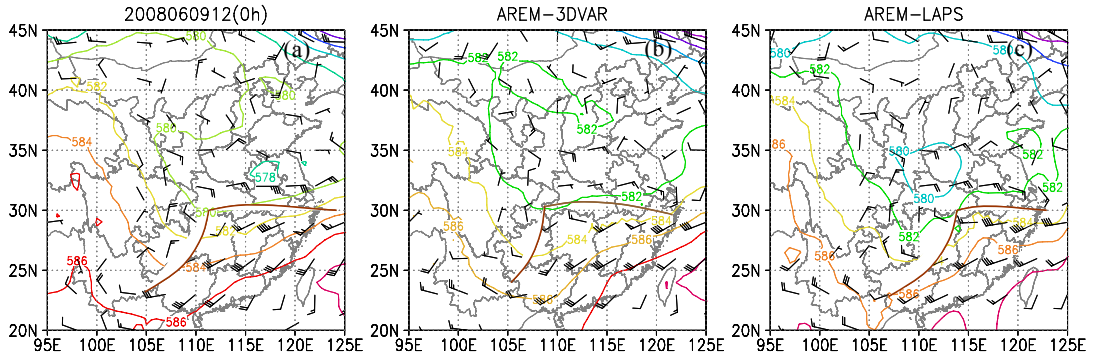

Figure 9. 700-hPa wind field and 500-hPa geopotential height field at 20:00 June 9, 2008. a. Observation; b. Exp. AREM-3DVAR; c. Exp. AREM-LAPS. Isoline unit: dgpm.

Both experiments simulated this vortex rainstorm process over South China fairly well, and their precipitation shapes, rain belt distribution, rain belt evolution, and center intensity corresponded to the observation fairly well. As for detailed description of rain belts, Exp. AREM-LAPS is superior to Exp. AREM-3DVAR. From 08:00 June 12 to 08:00 June 13, the 24-h strong precipitation centers were mainly in the central and northern part of Guangxi and the zone bordering southern Hunan and northwestern Guangdong, where extraordinary rainstorm occurred at 10 gauging stations (the strongest precipitation center was in Fuchuan, Guangxi with precipitation as high as 299.5 mm). This strong precipitation zone was simulated fairly successfully by both experiments, and the intensity simulated by Exp. AREM-3DVAR was of extremely heavy rain, while that simulated by Exp. AREM-LAPS was of extraordinary rainstorm, close to the observation. From 08:00 June 13 to 08:00 June 14, both experiments simulated the overall trend of the rain belt, but was not quite good in simulating the strongest extraordinary rainstorm belt in the coastal area of South China; both the simulated strong rain belts shifted northward, which might be related to the performance of the AREM model itself, which is to be further improved. However, as seen from comparison of the results between both experiments, the AREM-LAPS simulated intensity of the rain belt is close to the observation (Fig. 10).

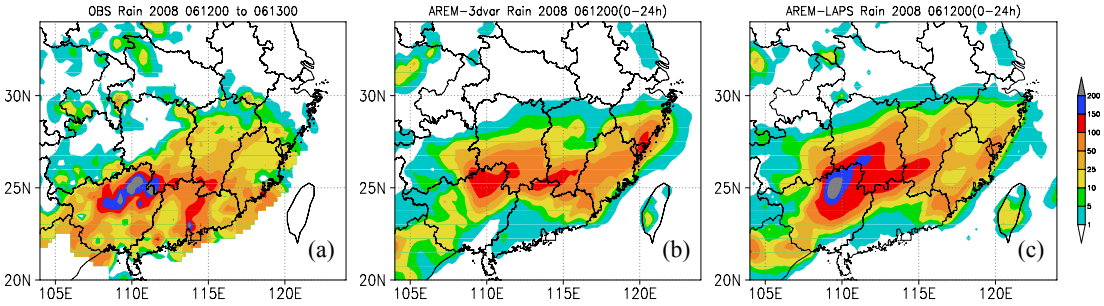

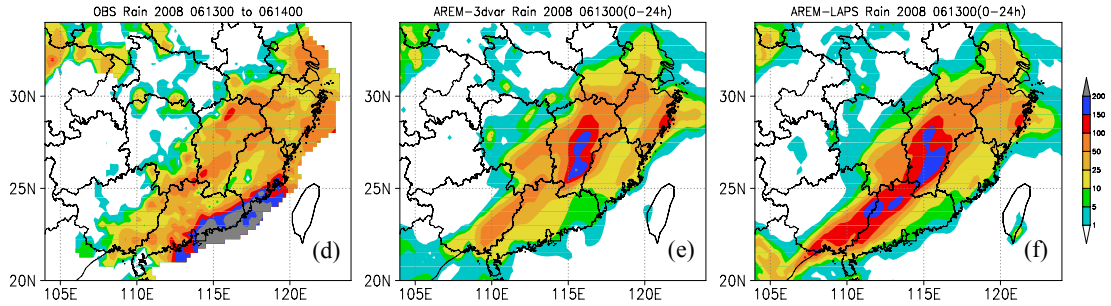

Figure 10. 24-h cumulative precipitation at 08:00 June 13-14, 2008 from the observation (a, d), AREM-3DVAR (b, e) and AREM-LAPS (c, f) experiments; unit: mm.

5.4.3 RAINSTORMS OVER YANGTZE-HUAIHE REGION ON JUNE. 21

From June 20 to 23, due to the influences of cold air and warm air as well as a mid-lower level Yangtze-Huaihe shear, rainstorms occurred successively in the Yangtze-Huaihe region. From 08:00 June 21 to 08:00 June 22, rainstorms mainly centered on the Dabie Mountains, with torrential rain to extremely heavy rain occurring in southern Henan, northeastern Hubei and central Anhui. The AREM-3DVAR simulated rain belt slightly shifted northward, and the simulated precipitation intensity for the Dabie Mountains was weak, with moderate to heavy rain generally and torrential rain at some points. However, Exp. AREM-LAPS fairly succeeded in simulating the extremely heavy rain over this region, and the simulated intensity and location were fairly close to the observation. Nevertheless, the intensity simulated by Exp. AREM-LAPS for the precipitation area in southwestern Hubei was somewhat strong and the precipitation simulated by Exp. AREM-3DVAR for southwestern Hubei remained weak (Fig. 11).

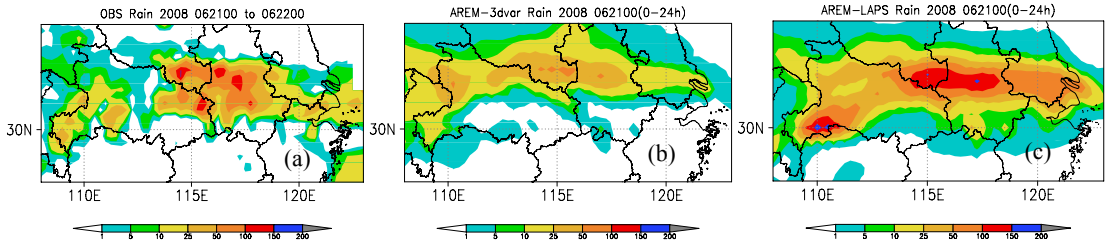

Figure 11. 24-h cumulative precipitation at 08:00 June 22, 2008. a. Observation; b. Exp. AREM-3DVAR; c. Exp. AREM-LAPS. Unit: mm.

It can be found by comparing the evolution of physical variables that, the main cause of the discrepancies in rain belt location and intensity between the two experiments is the simulation of the mid-lower shear in the Yangtze-Huaihe region. At the initial time, the stream fields of both experiments at 850 hPa did not differ much, exhibiting a vortex in the eastern part of Southwest China and a shear in the central Hubei and to the east of the vortex. Afterwards, their discrepancy gradually increased. By the 12th hour in model integration, the shear in Exp. AREM-3DVAR lay in southwestern Hubei to northwestern Hubei and then moved to southern Henan (Fig. 12a), while the shear in Exp. AREM-LAPS extended from northern Guizhou to southwestern Hubei and a plain south of the Yangtze River and then to northeastern Hubei all the way to central Anhui, the direction and speed of the wind on both sides of the shear were much stronger than those in Exp. AREM-3DVAR, and the shear position was more southward than that in Exp. AREM-3DVAR (Fig. 12b). By the 24th h in model integration, the shear simulated by Exp. AREM-LAPS (Fig. 12d) remained stable in the Yangtze-Huaihe region, with intensity and location improved over those simulated by Exp. AREM-3DVAR (Fig. 12c). The stream field difference led to great discrepancies in simulated rain belt location and intensity between these two experiments.

5.4.4 LOCAL EXTRAORDINARY RAINSTORM OVER SOUTHWESTERN HUBEI ON JULY 3

On July 3, owing to the influence of a mid-lower level vortex, one local extraordinary rainstorm took place in southwestern Hubei, where six gauging stations had torrential rains (extraordinary rainstorm at one station and extremely heavy rain at two stations), and the extraordinary rainstorm center was located at Jianshi, Hubei (109.72°E, 30.6°N, 220.9 mm). Exp. AREM-3DVAR simulated a northeast-southwest rain belt from southern

Shandong-northern Anhui-northern Jiangsu-Henan-northwestern Hubei, southwestern Hubei, to Jianghan Plain-Chongqing; not only the forecast of the rain belts in northern Anhui, northern Jiangsu, Henan, northwestern Hubei and Jianghan Plain by this experiment was null, but also the simulated intensity of extraordinary rainstorm over southwestern Hubei was obviously weaker, only at the grade of moderate rain. Exp. AREM-LAPS not only simulated the locality of this rainstorm process with the simulated precipitation area being very close to the observation, but also increased significantly the simulated intensity to 393 mm, higher than the real intensity, and the simulated precipitation center (110.5°E, 30°N) slightly shifted to the south and east (Fig. 13). To judge more accurately the simulation of this extraordinary rainstorm process by Exp. AREM-LAPS, we summed up the data of the intensive hourly rain gauging stations in Hubei Province collected from 09:00 July 3 to 08:00 July 4, 2008, and found that at Xiaoxikou power station (109.83°E, 30.56°N), about 13 km from the county seat of Jianshi, Hubei, the 24-h cumulative precipitation amounted to 428 mm; it is thus evident that the intensity and location of the Exp. AREM-LAPS simulated precipitation center further reduce their differences from the observation.

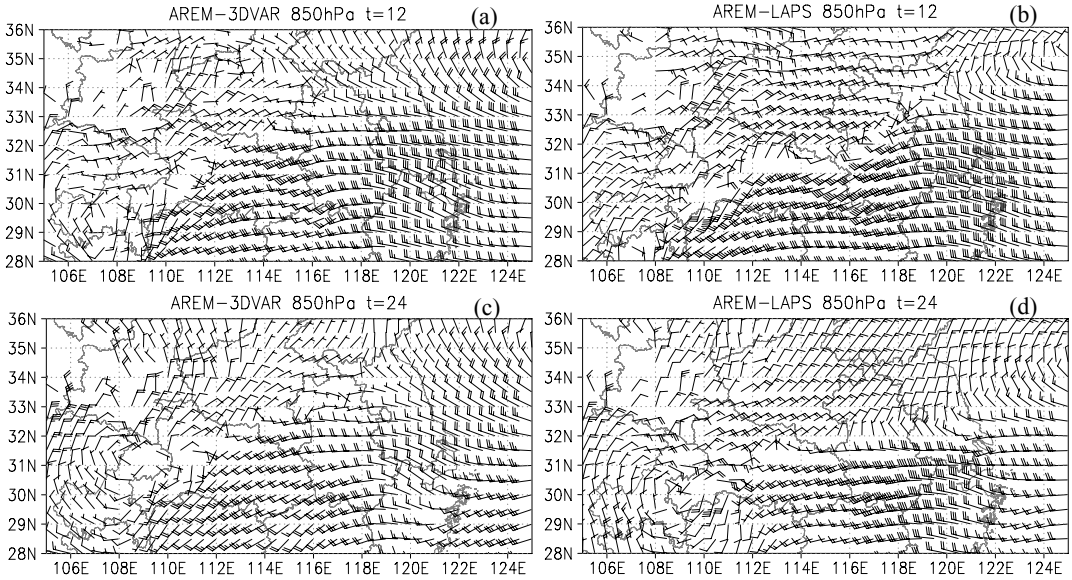

Figure 12. 850-hPa stream fields in AREM-3DVAR/AREM-LAPS experiments starting from 08:00 June 21, 2008 after integration for 12 h (a, b) and 24 h (c, d).

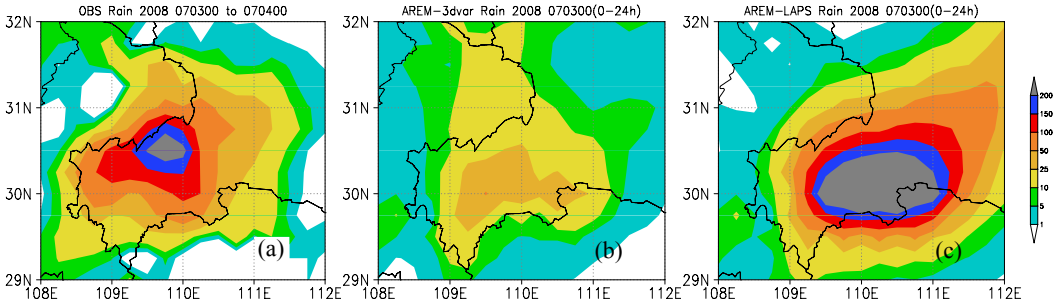

Figure 13. Similar to Fig. 11 but for 08:00 July 4, 2008.

After investigating the evolution of physical variables, we found that Exp. AREM-LAPS simulated this local extraordinary rainstorm process fairly successfully, because it simulated a very small scale, enclosed low-pressure system that remained stable at 850–700 hPa within the 4–24 h interval of model integration so that the location and intensity of the simulated 24-h extraordinary rainstorm center are very close to the observation. Simulation of local extraordinary rainstorms has always been difficult in numerical model prediction of mesoscale rainstorms. The process in this paper adopted the LAPS analysis as the initial field of the model and simulated the center of the 393-mm extraordinary rainstorm. Although not entirely as desired, its result is still exciting. Therefore, under suitable initial conditions, the AREM model has the capability of simulating a local extraordinary rainstorm process.

5.4.5 EXTENSIVE RAINSTORMS OVER CHINA ON JULY 5

On July 5, 2008, under the joint influences of a western Pacific subtropical high and a 500-hPa trough,

cold air and warm air converged in the southwest warm and humid air current are transported to the zone west of the subtropical high to form a northeast-southwest rain belt extending about 3000 km from northeast China, Beijing, Tianjin, Hebei to the Yunnan-Guizhou Plateau, with the main rainstorm zones centered on the northeastern and southwestern parts of China. For this extensive, systematic precipitation process, both experiments performed fairly well and simulated the precipitation that is close to the observation, but the rain belt intensities simulated by Exp. AREM-3DVAR were weak whereas those simulated by Exp. AREM-LAPS were close to the observation (Fig. 14).

It can be seen from the comparison of physical variables between the two experiments that their weather patterns are fairly similar at the initial time, the 500-hPa Eurasian mid-high level atmospheric circulation exhibits stable a "two-troughs versus one-ridge" pattern, with one low-pressure trough on the east side of the Ural Mountains and another in the eastern part of China, and a high-pressure ridge in the Lake Baikal region, where the water vapor was transported northward along a southwest air current before a main East Asian trough. The western Pacific subtropical high analyzed from the 500-hPa initial field in Exp. AREM-3DVAR (Fig. 15a) was obviously stronger than that analyzed in Exp. AREM-LAPS (Fig. 15b) and the real sounding data (figure omitted), so that fairly obvious change took place in the intensity of the main East Asian trough during model integration. It is discovered from the distribution of 500-hPa average wind field, average height field and 700-hPa average specific humidity field of the model in 0–24 h (Figs. 15c and 15d) that, despite that there is no much discrepancy in the locations of the main East Asian trough and water vapor transporting belt between the two experiments, both the average intensity and average specific humidity of the trough simulated by Exp. AREM-3DVAR are weaker than those simulated by Exp. AREM-LAPS, which is the very cause of the fact that the extensive rain belts in China simulated by both experiments have similar area and location but different intensity.

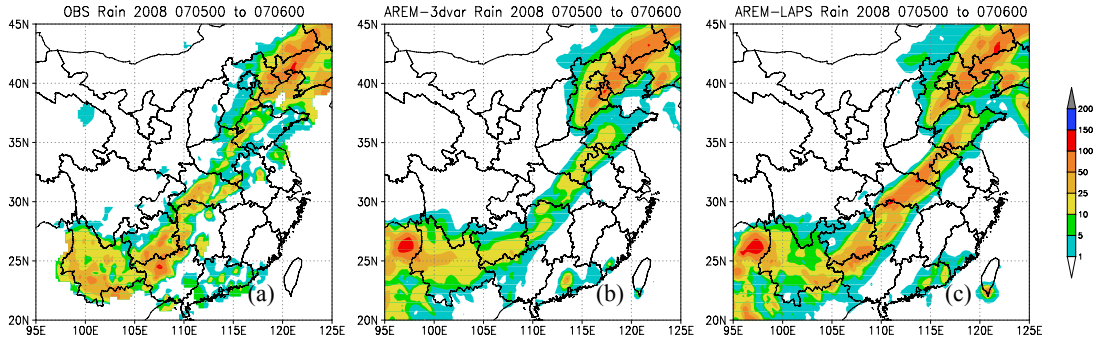

Figure 14. Similar to Fig. 11 but for 08:00 July 6, 2008.

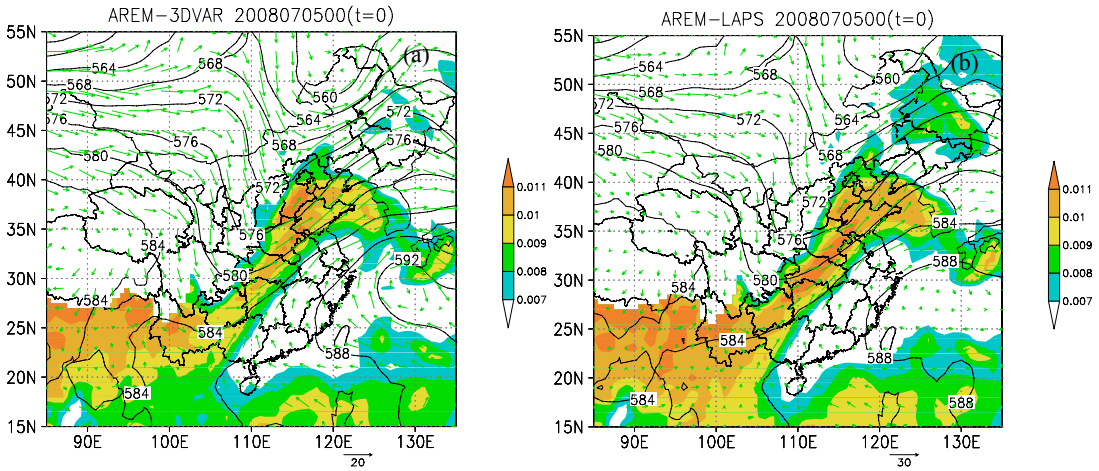

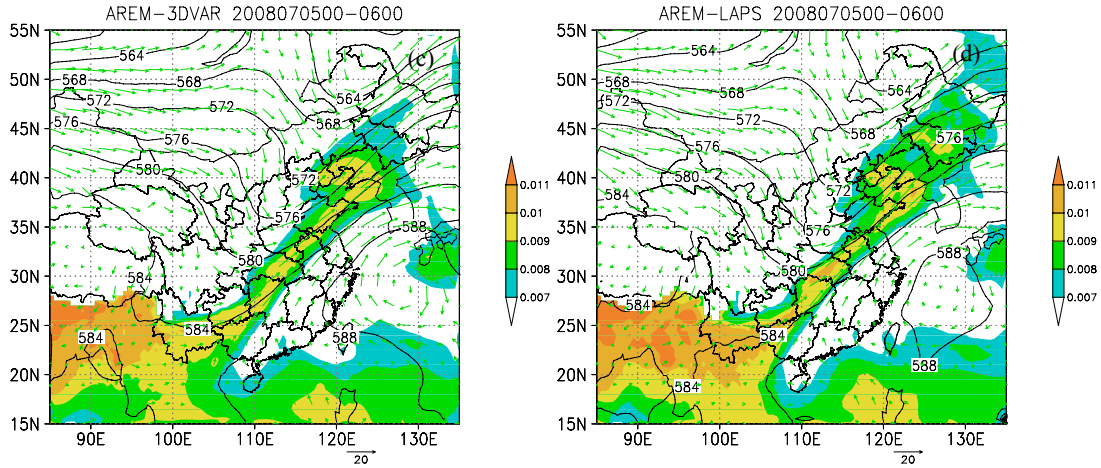

Figure 15. Initial field (a, b), 500-hPa average geopotential height field for 0-24 h of model integration (isolines, unit: dgpm), average wind field (unit: m/s) and 700-hPa average specific humidity field (shades, unit: kg/kg) (c, d) in AREM-3DVAR and AREM-LAPS at 08:00 July 5, 2008.

5.4.6 RAINSTORMS IN SHANDONG AND SOUTH CHINA ON JULY 18

From 08:00 July 18 to 08:00 July 19, strong precipitation was mainly distributed in two regions of China; one was from Taiwan, northeastern Guangdong, Fujian, southern Zhejiang to southern Jiangxi where torrential rain and extremely heavy rain generally occurred due to Typhoon Kalmaegi (No. 0807); the other was the most parts of Shandong province where heavy-to-torrential rain fell with extremely heavy rain-extraordinary rainstorm occurring in some parts of the province, due to the joint effects of vortex and peripheral circulation around Typhoon Kalmaegi. Exp. AREM-3DVAR basically predicted the precipitation over both of these regions, but with smaller area and weaker intensity of typhoon-caused precipitation, and simulated weaker intensity for the center of the Shandong rainstorm as well.

Both of the above aspects were somewhat improved by Exp. AREM-LAPS, which increased the center intensity of the Shandong rainstorm from 110 mm to 160 mm, and also increase both intensity and area of a typhoon-caused rainstorm region in South China coastal area to different extents (Fig. 16).

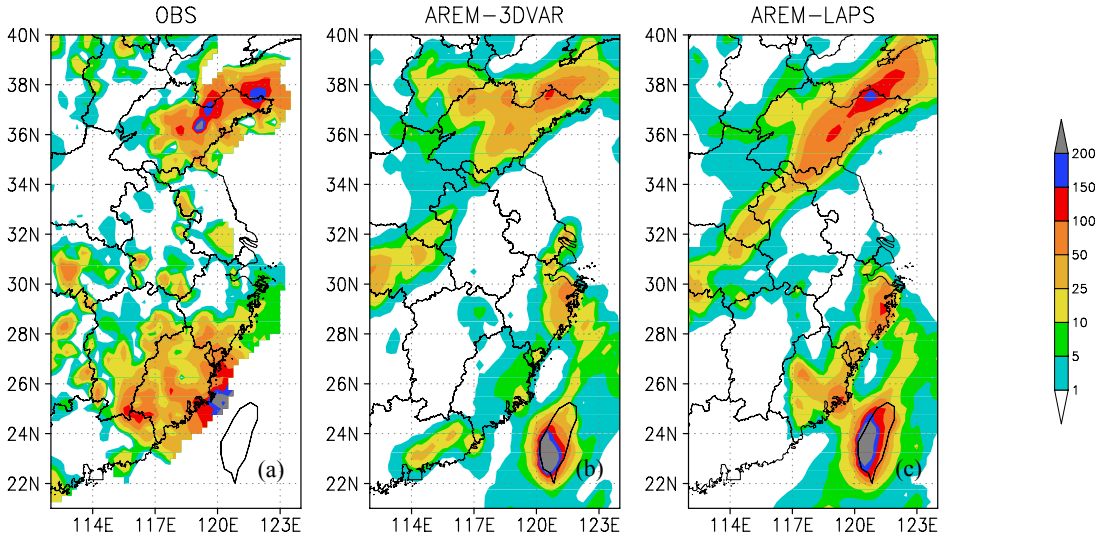

Figure 16. 24-h cumulative precipitation at 08:00 July 19, 2008. a. Observation; b. Exp. AREM-3DVAR; c. Exp. AREM-LAPS. Unit: mm.

6 CONCLUSIONS AND DISCUSSION

Influences of the AREM model on the simulation of the precipitation from May 22 to July 30, 2008 have been discussed using two different initialization schemes, LAPS and GRAPES-3DVAR, based on the same data source.

The results of TS score over the whole model integration region and subregions (the middle and

lower reaches of the Yangtze River, South China, North China, Northeast China and the eastern part of Southwest China) at five precipitation thresholds (light rain, moderate rain, heavy rain, torrential rain and extremely heavy rain) in five forecast time intervals (0–24 h, 12–36 h, 24–48 h, 36–60 h and 48–72 h) show that the TS scores of Exp. AREM-LAPS are generally higher than those of Exp. AREM-3DVAR, indicating that Exp. AREM-LAPS somewhat improves the effects of precipitation forecast for various regions, thresholds and validity periods in most cases.

Exp. AREM-3DVAR's general simulation of the average precipitation distribution was fairly approximate to the observation, but the forecast rain area has smaller scope and weaker intensity; Exp. AREM-LAPS obviously improves this and reproduces fairly well the precipitation area in the eastern China region, especially the major rain area in Guangxi and Guangdong, Fujian, Jiangxi and the Yangtze River Delta, with precipitation intensity roughly comparable to the observation.

For the simulation of temporal evolution of regional average precipitation, Exp. AREM-LAPS outperforms Exp. AREM-3DVAR in simulating north-south precipitation processes and precipitation intensity variation. However, in both experiments the simulated South China rain belt shifted northward, which might be related to the performance of the AREMv2.3 itself.

For the simulation of daily precipitation in major rain zones in China, including the eastern part of Southwest China, South China coastal area, the middle and lower reaches of the Yangtze-Huaihe Rivers basin, and Jiaodong Peninsula, Exp. AREM-LAPS outperforms Exp. AREM-3DVAR, with the former reproducing very well the enhancing and subsiding processes of daily mean precipitation rates in the above four regions, and the simulated intensities are roughly comparable to the observation. On the other hand, the intensities simulated by Exp. AREM-3DVAR are obviously weaker, especially in the eastern part of Southwest China.

In this study, comparative tests of more than ten typical precipitation processes during the summer of 2008 has been done, rainstorms occurring in different regions and due to different influential systems (extraordinary rainstorms over southern China arising from high-level troughs and mid-lower level intensive shears, vortex rainstorms over South China, Yangtze-Huaihe shear rainstorms, local extraordinary rainstorms caused by mid-lower level vortexes, 500-hPa troughs induced extensive rainstorms in China, typhoon-caused rainstorms, and torrential rains caused by vortices and peripheral circulation around the typhoon) have been investigated in detail, and the results indicate that Exp. AREM-LAPS predicts rain belt area, location and intensity better than the AREM-3DVAR, particularly so in precipitation intensity.

For capturing local precipitation centers with small horizontal scale due to local topographic effect, Exp. AREM-LAPS has certain advantages over Exp. AREM-3DVAR, but may overestimate the intensity of the precipitation center, which is to be validated in the future using precipitation data with higher spatial resolution.

LAPS is advantageous in including multiple types of observations, such as radar, satellite and GPS data, conveniently and quickly; the main purpose of this paper is to compare the influences of different initialization analysis schemes (LAPS and GRAPES-3DVAR) on precipitation forecast with the same data source adopted, in an attempt to offer references for operational application. The influences of applying radar, satellite and GPS data in the AREM-LAPS system on model precipitation forecast will be otherwise discussed in another paper.

REFERENCES:

[1] YU Ru-cong. The design of the limited area numerical weather prediction model with steep mountains [J]. Chin. J. Atmos. Sci., 1989, 13(2): 145-158.
[2] YU Ru-cong. Two-step shape-preserving advection scheme [J]. Adv. Atmos. Sci., 1994, A11 (4): 479-490.
[3] YU Ru-cong. Application of a shape-preserving advection scheme to the moisture equation in an E-grid regional forecast model [J]. Adv. Atmos. Sci., 1995, 12(1): 13-19.
[4] YU Ru-cong, XUE Ji-shan, XU You-ping, et al. An advanced regional Eta-coordinate numerical heavy-rain prediction model (AREM) system (AREMS) [M]. Beijing: China Meteorological Press, 2004: 45-49 (in Chinese).
[5] GONG Ying, WANG Ye-hong, LAI An-wei. Evaluation and analysis of rain prediction effect of three models in Southwest in 2008 [J]. Plateau Meteor., 2010, 29(6): 1441-1451 (in Chinese).
[6] YE Cheng-zhi, PAN Zhi-xiang, Cheng Rui, et al. The numerical research of the primary mechanism of the offing reinforcement of typhoon Rananim based on AREM [J]. Acta Meteor. Sinica, 2007, 65(2): 208-220 (in Chinese).
[7] LI Jun, WANG Ming-huan, GONG Ying, et al. Precipitation verifications to an ensemble prediction system based on AREM [J]. Torr. Rain Disast., 2010,29 (1): 30-37 (in Chinese).
[8] LI Jun, DU Jun, WANG Ming-huan, et al. Precipitation verifications to an ensemble prediction system using two initial perturbation schemes based on AREM [J]. J. Trop. Meteor., 2010, 26(6): 733-742 (in Chinese).
[9] ZHAO Yu-chun, WANG Ye-hong. Numerical study on the effect of topography upon "6·22" heavy rain in eastern Hubei [J]. Acta Meteor. Sinica, 2004, 62(Suppl.): 19-27 (in Chinese).
[10] WANG Ye-hong, WANG Zhi-bin. A test for real-time precipitation forecast during 2002-flood season with AREM model [J]. Meteor. Mon., 2005, 31(2): 17-22 (in Chinese).
[11] ZHANG Hua, XUE Ji-shan, ZHUANG Shi-yu, et al. Ideal experiments of GRAPES three-dimensional variational data assimilation system [J]. Acta Meteor. Sinica, 2004, 62(1): 31-41 (in Chinese).
[12] ZHAO Ying, WANG Bin. Numerical experiments for

typhoon Dan incorporating AMSU-A retrieved data with 3DVM [J]. Adv. Atmos. Sci, 2008, 25(4): 692-703 (in Chinese).
[13] MCGINLEY J A, ALBERS S C, STAMUS P A. Local data assimilation and analysis for nowcasting [J]. Adv. Space Res., 1992, 12(7): 179-188.
[14] ALBERS S C, MCGINLEY J A, BIRKENHUER D A, et al. The local analysis and prediction system (LAPS): Analysis of clouds, precipitation and temperature [J]. Wea. Forecast., 1996, 11(3): 273-287.
[15] LIU Zhi-xiong, DAI Ze-jun, PENG Ju-xiang, et al. Mechanism analysis of a local strong hail based on LAPS [J]. Torr. Rain Disast., 2009, 28(4): 313-320 (in Chinese).
[16] ZHOU Hou-fu, GUO Pin-wen, ZHAI Jing, et al. Application of LAPS analysis field in rainstorm mesoscale analysis [J]. Plateau Meteor., 2010, 29(2): 461-470 (in Chinese).
[17] CHEN Jia-rong, HUANG Wei-peng, WANG Wen-he, et al. Review of LAPS nowcasting system's forecasts in 2006 Mei-Yu and typhoon season [C]// Proc. 2007 Cross-Strait Meteorological Science and Technology Workshop. 2007: 114-120 (in Chinese).
[18] JIAN Guo-ji, MCGINLEY J A. Evaluation of a short-range forecast system on quantitative precipitation forecasts associated with tropical cyclones of 2003 near Taiwan [J]. J. Meteor. Soc. Japan, 2005, 83: 657-681.
[19] SNOOK J S, CRAM J M, SCHMIDT J M. LAPS/RAMS, A nonhydrostatic mesoscale numerical modeling system configured for operational use [J]. Tellus, 1995, 47A: 864-875.
[20] SHAW B L, THALER E R, SZOKE E J. Operational evaluation of the LAPS−MM5 "hot start" local forecast model[C]. 18th Conf. on Wea. Anal. and Forecast., Ft. Lauderdale: Amer. Meteor. Soc., 2001: 160-164.
[21] ETHERTON B, SANTOS P. Sensitivity of WRF Forecasts for South Florida to Initial Conditions [J]. Wea. Forecast., 2008, 23: 725-740.
[22] LI Hong-li, CUI Chun-guang, WANG Zhi-bin. Scientific designs, functions and applications of LAPS [J]. Torr. Rain Disast., 2009, 28(1): 64-70 (in Chinese).
[23] LI Hong-li, WAN Rong, XIE You-cai. Application of ground-based GPS water vapor in LAPS [J]. J. Trop. Meteor., 2010, 26(6): 702-709 (in Chinese).
[24] LI Guo-jing, XU You-ping, CHENG Wei, et al. Doppler radar data assimilation sensitivity experiment on a heavy rain event [J]. Torr. Rain Disast., 2009, 28(2): 97-103 (in Chinese).
[25] WANG Yu. Verification of NMC subjective and objective precipitation prediction during the main flood season in 2002 [J]. Meteor. Mon., 2003, 29(5): 21-25 (in Chinese).
[26] WANG Yu, YAN Zhi-hui. Effect of different verification schemes on precipitation verification and assessment conclusion [J]. Meteor. Mon., 2007, 33(12): 53-61 (in Chinese).
[27] WANG Ye-hong, ZHAO Yu-chun, ZHANG Bing. Verifications of precipitation forecasts from advanced AREMS during 2003 flood season [J]. J. Trop. Meteor., 2005, 21(6): 597-604 (in Chinese).
[28] GONG Ying. Evaluation and analysis of the rainfall prediction of AREM in flood season of 2007 [J]. Torr. Rain Disast., 2007, 26(4): 372-380 (in Chinese).
[29] YANG Jing-an, MENG Ying-jie. Main heavy rain process in China during May to September in 2008 [J]. Torr. Rain Disast., 2008, 27(4): 378-382 (in Chinese).
[30] YANG Jing-an, MENG Ying-jie. Main heavy rain process in China during May to September in 2008 (continue) [J]. Torr. Rain Disast., 2008, 28(1): 92-95 (in Chinese).

Citation: WANG Ye-hong, PENG Ju-xiang and ZHAO Yu-chun. Numerical experiments for the effects of two model initialization schemes on rainfall forecast in the 2008 flooding season. *J. Trop. Meteor.*, 2014, 20(3): 251-266.